Materials and Design 106 (2016) 463–475

Contents lists available at ScienceDirect

Materials and Design

journal homepage: www.elsevier.com/locate/matdes

Microstructural evolution and mechanical properties of the stir zone in friction stir processed AISI201 stainless steel

H.B. Cui [a], G.M. Xie [a,*], Z.A. Luo [a], J. Ma [a], G.D. Wang [a], R.D.K. Misra [b]

[a] State Key Laboratory of Rolling and Automation, Northeastern University, No. 3 Wenhua Road, Shenyang 110819, China
[b] Department of Metallurgical, Materials, and Biomedical Engineering, University of Texas at El Paso, TX 79968, USA

ARTICLE INFO

Article history:
Received 14 April 2016
Received in revised form 26 May 2016
Accepted 27 May 2016
Available online 29 May 2016

Keywords:
Friction stir processed
AISI201 stainless steel
Grain structure
Recrystallization
δ-Ferrite
Sigma phase
Mechanical properties

ABSTRACT

AISI 201 stainless steel plate was friction stir processed (FSP) at rotation speeds in the range of 500–1000 rpm with traverse speed of 100 mm/min, and rotation speed of 1000 rpm with traverse speed of 50 mm/min using W-Re stirring tool. The microstructural evolution was studied by optical microscopy, scanning electron microscopy, electron backscattered diffraction, electron probe micro analyzer and transmission electron microscopy. The results suggested that the final grain structure in the stir zone (SZ) originated from the competition between continuous recrystallization (CDRX) and discontinuous recrystallization (DDRX). The grain size and the content of δ-ferrite in SZ were closely related to the processing parameters, and a band structure contained 6.5% δ-ferrite formed. Furthermore, the δ-ferrite formed in SZ significantly promoted the occurrence of DDRX and strong (111)[112] annealing texture formed in δ-ferrite. No sigma phase was observed in the SZ, and the density of dislocations and sub-structures was found to be seriously affected by the processing parameters and locations of SZs. The relationship between mechanical properties and structure is elucidated.

1. Introduction

Austenitic stainless steels are widely used in industrial manufacturing for a wide range of applications from kitchen ware and furniture to sophisticated equipment [1]. According to the American Iron and Steel Institute (AISI) classification, the austenitic stainless steel grades are designated by numbers such as 200 (Fe–Cr–Ni–Mn–N system with ≥2 wt.% Mn) and 300 series (Fe–Cr–Ni system ≤2 wt.% Mn). AISI201 is a typical 200 series austenitic stainless steel, in which nickel element is replaced by austenite stabilizing elements, nitrogen and manganese. It is well established that nitrogen not only improves the strength and fracture toughness of stainless steel, but also enhances the local corrosion resistance, especially the pitting and crevice corrosion resistance [2]. In addition, saving in nickel content reduces the cost of stainless steels. Luo et al. [3] noted that the price of AISI 201 was only one third of 316L austenitic stainless steel. However, several difficulties were experienced during fusion welding of austenitic stainless steels, such as hot crackling sensitivity and vaporization of element etc. Furthermore, grain growth occurred and detrimental precipitates formed in the weld zones was hardly prevented [4,5]. In order to avoid these problems, friction stir welding (FSW) was utilized to join austenitic stainless steels. During FSW, a rotating tool with a special designed pin and shoulder was inserted into the plates and traversed along the edge line of the joint. Heat was generated by friction between the tool and plate, and material was heated and stirred by the tool. This technology was initially applied to aluminum alloys and magnesium alloys, with the development of stirring tool, FSW was applied to join higher melting point alloys and producing joints with high-quality [6–9]. Furthermore, the dissimilar alloys were also joined by FSW [10–12].

Recently, based on the basic principles of FSW, friction stir processing (FSP) was developed for microstructural modification of metallic materials. Currently, several studies focused on FSP/FSW austenitic stainless steels [5,13–21,56]. Sabooni et al. [5] investigated the microstructural evolution during FSP 304L stainless steel. Hajian et al. [14] refined 316L stainless steel at low rotational speeds using FSP, and the grain size in SZs was decreased to 0.8–2.2 μm. Similarly, the grain refinement by FSP was also applied to coating on 316L austenitic stainless steel [15]. Mehranfar et al. [13] noted that nanostructure surface was produced during FSP super-austenitic stainless steel [13]. On the other hand, Wang et al. [16] and Miyano et al. [17] conducted FSP/FSW of high nitrogen austenitic stainless steel, and the tensile mechanical properties of the joint were excellent. Miura et al. [18] found that the austenite phase in SZ was stabilized after FSW. Grain structure development during FSW 316 austenitic stainless steel was studied by Jeon et al. [19], and they found out that material flow was close to simple shear deformation and the final texture was dominated by simple shear texture. A number of reports indicated that the sigma phase, which was detrimental to the mechanical properties, usually formed in FSP/FSW austenitic stainless steels [20–23]. Nevertheless, the formation of

* Corresponding author.
E-mail address: gmxieneu@126.com (G.M. Xie).

http://dx.doi.org/10.1016/j.matdes.2016.05.106
0264-1275/

Table 1
Nominal chemical composition of AISI 201stainless plate (wt.%).

C	Si	Mn	Si	Cr	Ni	Mo	Cu	N	Fe
0.067	0.42	8.2	0.376	18.3	4.82	0.02	1.82	0.175	Bal.

sigma phase was successfully prevented through optimizing processing parameters [14,17].

Based on the above studies, the mechanical properties and microstructural evolution in SZs during FSP/FSW austenitic stainless steels were closely related to processing parameters [5,13–23,56], but the processing parameters in previous studies were limited. Furthermore, there are a few studies on FSP AISI201 stainless steel that have been reported. In this study, AISI201 austenitic stainless steel was subjected to FSP using different processing parameters. The objective of this study is to elucidate the microstructural evolution and mechanical properties in FSP AISI201steel in a systematic manner.

2. Experimental procedure

In our study, 4.4 mm thickness AISI 201 stainless plate was friction stir processed at rotation speed of 500, 800, 1000 rpm with traverse speed of 100 mm/min, and 1000 rpm with traverse speed of 50 mm/min using W-Re stirring tool. The plate's nominal chemical composition is listed in Table 1. The W-Re (nominal composition W-25 wt.% Re) stirring tool equipped with a columnar shape pin of 3 mm diameter with thread and 20 mm diameter shoulder was used. The tool tilt angle was set at 3° from the nominal direction of the plate. The metallurgical inspection was performed on the cross-section of the processed samples perpendicular to the FSP direction. The specimens for optical microscopy (OM) and scanning electron microscopy (SEM) were etched in a solution of 10% oxalic acid and 90% water at 30 V. The phase and texture analysis in the SZs were carried out using electron backscattered diffraction (EBSD) technique. The specimen for EBSD was prepared by electrolytic polishing with a 10% perchloric acid and 90% ethanol solution at 30 V. As shown in the boxes in Fig. 1(b), the EBSD testing studies were carried out on the AS and RS, respectively. Elemental distribution was characterized by JEOL5853-type electron probe micro analyzer (EPMA) equipped with an energy-dispersive spectroscopy (EDS) analysis system. Thin foils for transmission electron microscopy (TEM) were prepared by twin jet-polishing in 10% perchloric acid. The mechanical properties were evaluated using Vickers hardness and transverse tensile test. The hardness values of the transverse section were measured at the distance of about 1 mm from the surface of the FSP samples. Tensile properties of the FSP samples were determined using the tensile specimen machined perpendicular to the FSP direction at a constant crosshead speed of 1 mm/s. The dimensions of tensile samples are present in Fig. 2.

3. Results and discussion

3.1. Macrostructural analyses

The base metal exhibited as-annealed coarse grains in the range from 30 to 80 μm and contained some typical annealing twins (Fig. 3). Fig. 1(a) shows the typical transverse cross-section of the FSP sample. Three distinct regions are identified as stir zone (SZ), thermo-mechanically affected zone (TMAZ) and base metal (BM) (Fig. 1(b)). Due to the severe plastic deformation and frictional heating during FSP, the SZs exhibited a symmetric basin-like shape. No obvious heating affected zone was found and a very clear boundary located between AS and TMAZ was observed. Furthermore, a special band structure (BS) formed on the AS of sample 1000 rpm–100 mm/min (Fig. 1(a)). Fig. 4(a) shows an illustration of BS, and a void defect formed closed to the BS (Fig. 4(b)).

3.2. Microstructural analysis

3.2.1. The mechanism of dynamic recrystallization

It was revealed that the material in the SZ of FSP experienced extreme plastic deformation and thermal exposure, which resulted in significant microstructural refinement and homogeneity of SZ due to dynamic recrystallization (DRX) [1]. In order to identify the mechanism of DRX in SZs during FSP AISI201 stainless steel, the EBSD results were analyzed. Grains boundary characteristic obtained by EBSD are presented in Fig. 5, where the low angle grain boundaries (LAGBs), i.e. grain boundary misorientation of 2–15°, and high angle grain boundaries (HAGBs), i.e. greater than 15°, are represented with green and black lines, respectively. The δ-ferrite is identified in red color. Fig. 6 showed the fraction of LAGBs and HAGBs at different locations of SZs. It was seen from Fig. 6 that the fraction of LAGBs on the advancing side (AS) of sample 800 rpm–100 mm/min was as high as 43.3%, and sub-structures were observed to a significant extent (Fig. 5(b)). Nevertheless, the fraction of LAGBs on the AS of sample 1000 rpm–100 mm/min was as low as 8.9% (Fig. 6), and only a small degree of sub-structures were observed (Fig. 5(c)). The texture component was also studied to investigate the microstructural evolution. According to the approach adopted by Mironov et al. [27], the process geometry was transformed into the ideal simple shear reference frame because the deformation during FSP/FSW was simple shear [5,6,8]. Fig. 7 showed inverse pole figure (IPF) map and orientation distribution function (ODF) on the AS

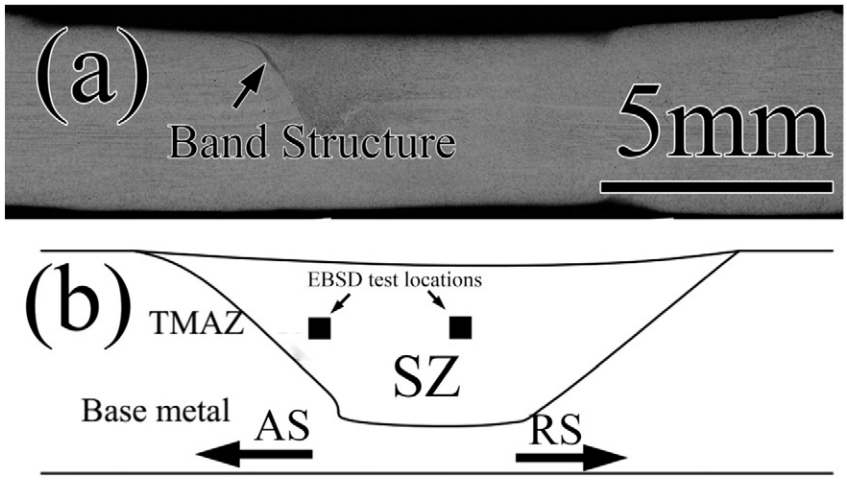

Fig. 1. Typical macrostructure of FSP sample of (a) 1000 rpm–100 mm/min and (d) schematic illustration.